

Rho-Kinase Inhibition Blunts Renal Vasoconstriction Induced by Distinct Signaling Pathways *In Vivo*

ALESSANDRO CAVARAPE,* NICOLE ENDLICH,[†] ROBERTA ASSALONI,*
ETTORE BARTOLI,[‡] MICHAEL STEINHAUSEN,[†] NIRANJAN PAREKH,[§] and
KARLHANS ENDLICH[†]

*Department of Experimental and Clinical Pathology and Medicine (DPMSC), University of Udine, Udine, Italy; [†]Department of Anatomy and Cell Biology, University of Heidelberg, Heidelberg, Germany;

[‡]Department of Clinical Pathology and Medicine, University of Piemonte Orientale, Novara, Italy; and

[§]Department of Physiology and Pathophysiology, University of Heidelberg, Heidelberg, Germany.

Abstract. In addition to intracellular calcium, which activates myosin light chain (MLC) kinase, MLC phosphorylation and hence contraction is importantly regulated by MLC phosphatase (MLCP). Recent evidence suggests that distinct signaling cascades of vasoactive hormones interact with the Rho/Rho kinase (ROK) pathway, affecting the activity of MLCP. The present study measured the impact of ROK inhibition on vascular F-actin distribution and on vasoconstriction induced by activation/inhibition of distinct signaling pathways *in vivo* in the microcirculation of the split hydronephrotic rat kidney. Local application of the ROK inhibitors Y-27632 or HA-1077 induced marked dilation of pre- and postglomerular vessels. Activation of phospholipase C with the endothelin ET_B agonist IRL 1620, inhibition of soluble guanylyl cyclase with 1H-[1,2,4]oxadiazolo-[4,3-a]quinoxalin-1-one (ODQ), or inhibition of adenylyl cyclase with the adenosine

A₁ agonist N⁶-cyclopentyladenosine (CPA) reduced glomerular blood flow (GBF) by about 50% through vasoconstriction at different vascular levels. ROK inhibition with Y-27632 or HA-1077, but not protein kinase C inhibition with Ro 31-8220, blunted ET_B-induced vasoconstriction. Furthermore, the reduction of GBF and of vascular diameters in response to ODQ or CPA were abolished by pretreatment with Y-27632. ROK inhibitors prevented constriction of preglomerular vessels and of efferent arterioles with equal effectiveness. Confocal microscopy demonstrated that Y-27632 did not change F-actin content and distribution in renal vessels. The results suggest that ROK inhibition might be considered as a potent treatment of renal vasoconstriction, because it interferes with constriction induced by distinct signaling pathways in renal vessels without affecting F-actin structure. *alessandro.cavarape@dpmc.uniud.it*

The primary signal for vascular smooth muscle cell (VSMC) contraction is an increase of intracellular calcium (Ca²⁺) levels, activating myosin light chain (MLC) kinase, which leads to MLC phosphorylation (1). In the past few years, evidence has accumulated that enhancement of Ca²⁺ sensitivity of VSMC, involving inhibition of MLC phosphatase (MLCP), contributes to VSMC contraction importantly (2). So far, two molecular mechanisms of MLCP inhibition have been uncovered (3). First, receptor-mediated activation of the small G protein RhoA leads to activation of Rho kinase (ROK), which inhibits MLCP through phosphorylation of its regulatory subunit either directly or via ZIP-like kinase (4,5). Second, protein kinase C α and δ isoforms have been identified to phosphorylate CPI-17, which, in the phosphorylated state, inhibits MLCP specifically (6,7). A recently developed ROK inhibitor, the pyridine

derivative Y-27632, has been shown to potently inhibit the contraction of preparations from experimental animals and human arterial vessels induced by different agonists *in vitro* and also to correct arterial pressure to normotensive levels in different experimental models of hypertension *in vivo* (8–11). Because of the evidence that the Rho/ROK pathway mediates tonic vasoconstriction, ROK is thought to play a crucial role in human diseases, *e.g.*, in hypertension and myocardial ischemia (12,13). The contribution of the ROK pathway to renal vasoconstriction is practically unknown.

A number of investigations have elucidated the role of a wide variety of circulating and locally produced vasoactive molecules in regulating renal hemodynamics under normal and pathologic conditions (14). Vasoconstrictors bind to specific receptors to activate intracellular pathways triggering contraction of VSMC. Also in the kidney, VSMC tone is regulated by a complex network of constricting and dilating intracellular signaling cascades, some of which might modulate vasomotor tone in part independent of changes in intracellular Ca²⁺. Thus, renal vasoconstrictors could increase Ca²⁺ sensitivity through MLCP inactivation mediated by ROK. Conversely, VSMC relaxation mediated by an increase in intracellular cAMP and cGMP is associated with a decrease of Ca²⁺ sensitivity (3,15). Evidence has accumulated that cGMP- and cAMP-dependent protein kinases can directly increase the activity of MLCP and

Received February 25, 2002. Accepted August 19, 2002.

Correspondence to Dr. Alessandro Cavarape, Department of Experimental and Clinical Pathology and Medicine (DPMSC), Chair of Internal Medicine, Piazza S. Maria della Misericordia, 1, 33100 Udine, Italy. Phone: 39-0432-559815; Fax: 39-0432-42097; E-mail: alessandro.cavarape@dpmc.uniud.it

1046-6673/1312-0037

Journal of the American Society of Nephrology

Copyright © 2002 by the American Society of Nephrology

DOI: 10.1097/01.ASN.0000039568.93355.85

interfere with the Rho/ROK pathway (3). However, the role of ROK in renal vasoconstriction mediated by distinct signaling pathways has not yet been investigated.

In addition to smooth muscle contraction, the Rho/ROK pathway stimulates stress fiber formation and actin polymerization in cultured cells (16). Accordingly, ROK inhibition with Y-27632 completely abolished stress fibers in cultured cells (11). Though actin filament disruption has been demonstrated to severely impair vasoconstriction in isolated mesenteric arteries (17), F-actin distribution in vessels has not yet been examined after ROK inhibition.

The aim of this study was to assess the influence of ROK on renal vasoconstriction at the microvascular level utilizing the *in vivo* model of the split hydronephrotic rat kidney. We employed different approaches to induce vasoconstriction through distinct intracellular pathways, namely phospholipase C activation, and reduction of intracellular cGMP or cAMP levels. Drug-induced constrictions in different renal vascular segments and reductions in glomerular blood flow (GBF) were measured under control conditions and after local application of the ROK inhibitors Y-27632 and HA-1077 as compared with PKC inhibition. Moreover, we also investigated the effect of ROK inhibition on actin filament organization in the renal vascular wall.

Materials and Methods

Preparation of the Hydronephrotic Kidney

The study protocols were performed on 29 female Wistar rats (210 to 240 g) in accordance with national animal protection guidelines. The animals had free access to food and water before the experiments. The technique and experimental procedures have been previously described in detail (18). Briefly, unilateral surgical hydronephrosis was induced by permanently ligating the left ureter via a flank incision during pentobarbital sodium anesthesia (Nembutal, 60 mg/Kg intraperitoneally; Ceva, Bad Segeberg, Germany). The final experiments were performed under thiobutabarbital anesthesia (Inactin, 100 mg/kg intraperitoneally; Byk Gulden, Konstanz, Germany) 2 to 3 mo after induction of hydronephrosis. Each rat was placed on a 37°C heated surgical table. The trachea was intubated, and the left jugular vein was cannulated for the continuous replacement of isotonic saline at a rate of 60 μ l/min and for infusion of drugs. A polyethylene catheter was inserted into the left femoral artery for continuous measurements of systemic BP. The left hydronephrotic kidney was exposed through a flank incision and split carefully along the great curvature using a thermal cautery. The dorsal half of the split kidney was sutured to a semicircular-shaped wire frame. Blood supply and innervation remained intact after this preparation. The wire frame with the fixed split kidney was placed at the bottom of a specially designed Plexiglas chamber suitable for intravital transillumination microscopy. The entry of the renal hilus into the chamber was sealed with silicon grease, and the chamber was filled with 50 ml of an isotonic, isocolloidal solution (Hemacel; Behringwerke AG, Marburg, Germany) maintained at a constant temperature of 37°C with a feedback-controlled heating system.

Videomicroscopy

The table was mounted on the microscope stage. Images of renal microvessels obtained through a special water-immersion objective (Ultrapak UO-55; Leitz, Wetzlar, Germany) were visualized with a

CCD camera, displayed on a calibrated monitor by a closed circuit TV system, and recorded on line on videotape. The luminal vessel diameters were measured directly from the monitor and were converted to *in vivo* diameters (expressed in micrometers) using a conversion factor to account for the magnification of the vessel images.

Vessel Segments and GBF

Measurements of the following vessel segments were carried out according to their branching pattern from the selected glomerulus: (1) proximal interlobular artery (near the arcuate artery); (2) distal interlobular artery (near the afferent arteriole); (3) proximal afferent arteriole (near the interlobular artery); (4) distal afferent arteriole (at a site within 100 μ m from the glomerulus); and (5) efferent arteriole (within 50 μ m from the glomerulus).

Velocity of red blood cells was measured in the efferent arteriole of the selected glomerulus by using a velocity-tracking correlator (Model 102B; IPM Inc., San Diego, CA). In this on-line computing system two photodiodes obtain photometric signals from the moving red blood cells (19). To obtain the GBF value, the measured red cell velocity was multiplied by the luminal cross-section of the efferent arteriole and corrected for the Fahreus-Lindqvist effect (20).

Experimental Protocols

After the surgical procedure, each kidney was allowed to adapt to the tissue bath conditions for at least 60 min. The stability of the preparation has been demonstrated for a duration of 3 h (21). Each protocol included several experimental periods at the end of which mean arterial pressure (MAP), vascular diameters, and GBF were measured. The first period served as baseline control.

Six series of experiments were performed. In the first series, dose-response experiments for Y-27632 were conducted. The other five experimental series started with control measurements during which the ET_B receptor agonist IRL 1620 (group 1, *n* = 6; group 2, *n* = 5; group 3, *n* = 5), the guanylyl cyclase inhibitor ODQ (group 4, *n* = 6) or the selective A₁ adenosine receptor agonist N⁶-cyclopentyladenosine (CPA) (group 5, *n* = 7) were locally administered into the tissue bath to reduce GBF from a threshold value to about 50% by up to three sequentially increasing doses of vasoconstrictors. After wash out (30 min) and baseline measurements in the five experimental series, measurements were taken after intrarenal inhibition of ROK by local administration of the selective inhibitors Y-27632 or HA-1077 or after intrarenal inhibition of PKC by local administration of Ro 31–8220. After control measurements, during which the renovascular parameters were evaluated in a new baseline condition at the steady state, the effects of IRL 1620, ODQ, and CPA were assessed after intrarenal inhibition of ROK or PKC, whereby the doses of IRL 1620 and CPA were augmented in groups 1, 4, and 5 to obtain a reduction in GBF comparable to that detected during the pre-inhibition measurements. Measurements were taken about 10 min after application of IRL 1620 and CPA and about 15 min after application of ODQ, Y-27632, HA-1077, and Ro 31–8220, when a steady state had been reached.

For stimulation of PLC, the ET_B agonist IRL 1620 was chosen, because we have demonstrated earlier that IRL 1620 induces not only preglomerular vasoconstriction but also marked efferent arteriolar constriction (22). The effects of IRL 1620 and of A₁ receptor agonists have been shown to be fully reversible after washout (22–24). Furthermore, vasoconstrictions induced by IRL 1620 and A₁ receptor agonists do not desensitize in the hydronephrotic kidney, as is the case for angiotensin II and diadenosine polyphosphates (22–26). The reversibility of the ODQ-induced vasoconstriction was confirmed by

wash out. To exclude that the renal vasculature desensitized in response to ODQ, the protocol was reversed (Y-27632 + ODQ, wash-out, ODQ) in half of the experiments. We obtained similar results for ODQ with the normal and the reversed protocol; therefore, data were pooled together.

Y-27632 and HA-1077 have been reported to inhibit ROK with IC_{50} values of $8 \cdot 10^{-7}$ M and $2 \cdot 10^{-6}$ M, respectively (27). Concentrations of 10^{-5} M Y-27632 and $2 \cdot 10^{-5}$ M HA-1077 inhibit PKC α by 2% and 14%, respectively (27). The IC_{50} value of Ro 31-8220 for PKC α inhibition is $3 \cdot 10^{-8}$ M, whereas 1 μ M Ro 31-8220 reduces ROK activity by only 8% (27).

It should be noted that the concentrations of vasoactive drugs, which are locally administered into the tissue bath, need to be about tenfold higher to elicit similar effects in the hydronephrotic kidney as compared with isolated or perfused preparations. For example, 10^{-9} M ET-1 and 10^{-8} M angiotensin II in the tissue bath constrict afferent arterioles by about 15%, whereas a similar diameter reduction is seen with 10^{-10} M ET-1 and $<10^{-9}$ M angiotensin II in isolated rat afferent arterioles (28) or in isolated perfused hydronephrotic kidneys (29,30). There is most likely a steep concentration gradient for locally applied drugs between the tissue bath and the vessel lumen, because the hydronephrotic kidney has a considerable thickness (200 to 400 μ m) and the concentration of drugs in the blood stream is practically zero.

IRL 1620 (Alexis, Germany), CPA (Boehringer Mannheim, Germany), Y-27632 (kindly provided by Yoshitomi Pharmaceutical Inc.), and HA-1077 (Alexis, Germany) were dissolved in saline. ODQ and Ro 31-8220 (Alexis, Germany) were dissolved in DMSO; the final DMSO concentration in the tissue bath was below 0.1%. All the vasoactive drugs used in our experiments were administered into the tissue bath by local application to avoid any systemic effect on hemodynamic parameters.

Examination of F-Actin Distribution

Hydronephrotic kidneys were prepared for videomicroscopy as described above. Hydronephrotic kidneys were incubated with either vehicle (controls) or 10^{-4} M Y-27632 for 30 min. Hydronephrotic kidneys were then excised and fixed in 2% paraformaldehyde for 2.5 h. The kidney tissue was cut in stripes, dehydrated in isopentane in liquid nitrogen, and mounted on styropor snips for cryosectioning. Kidney tissue was sectioned at 15- μ m thickness. Further procedures were identical to those as recently described (31). Briefly, sections were permeabilized (0.3% Triton X-100), blocked for 1 h at room temperature in blocking solution (2% fetal bovine serum, 2% bovine serum albumin, 0.2% fish gelatin in phosphate buffered saline), and incubated with Alexa-conjugated phalloidin (Molecular Probes, Eugene, OR) to visualize F-actin. Specimen were viewed with a confocal laser scanning microscope (TCS-SP; Leica Microsystems, Heidelberg, Germany). To assess F-actin intensity, all images were taken with identical confocal microscope settings for laser power, photo-multiplier gain, and pinhole size.

Statistical Analyses

Data are presented as mean \pm SEM. Changes in vascular diameters and GBF are expressed as percentage changes from the preceding control values. Paired and unpaired *t* test, ANOVA, and Bonferroni's method for multiple comparisons were used as appropriate to test for statistical significance. The data have been analyzed both as absolute and percent values. Values of $P < 0.05$ were considered statistically significant.

Results

Absolute values for measured parameters in five experimental groups under control conditions before and after application of inhibitors are listed in Table 1. MAP was not affected by local administration of vasoconstrictors or inhibitors in all the experimental groups, and it remained stable throughout the experimental protocols if not otherwise indicated.

Effects of ROK and PKC Inhibitors on Basal Vessel Tone

In the first series of experiments, the effect of increasing concentrations of the ROK inhibitor Y-27632 (10^{-7} to 10^{-4} M) on the spontaneous, endogenous tone of the interlobular artery was determined (Figure 1A). In the interlobular artery, diameter did not change at 10^{-7} and 10^{-6} M Y-27632, but it significantly increased at higher concentrations (10^{-5} and 10^{-4} M). The vascular pattern of dilation in response to the ROK inhibitor Y-27632 (10^{-4} M) was obtained from the pooled data of three groups of experiments (Figure 1B). Dilation was observed preferentially in preglomerular vessels, *i.e.*, in interlobular arteries and in proximal afferent arterioles. Efferent arterioles also dilated significantly in response to the ROK inhibitor Y-27632. Y-27632 almost doubled GBF.

The structurally different ROK inhibitor HA-1077 (10^{-4} M) reduced the spontaneous tone in pre- and postglomerular vessels to a similar degree as Y-27632 (Figure 2). However, dilation of the distal interlobular artery in response to the ROK inhibitor HA-1077 was somewhat weaker as compared with Y-27632-induced dilation. Pre- and postglomerular dilation in response to the PKC inhibitor Ro 31-8220 further revealed the involvement of PKC in the spontaneous tone of renal vessels (Figure 2). Although PKC inhibition dilated efferent arterioles as effectively as the ROK inhibitors, dilation of the distal interlobular artery in response to the PKC inhibitor was clearly less.

Effects of ET_B Receptor Agonist (IRL 1620), Guanylyl Cyclase Inhibitor (ODQ), and Adenosine A_1 Receptor Agonist (CPA)

The effects of local application of IRL 1620, ODQ, and CPA on luminal diameters and on GBF in hydronephrotic rat kidneys are depicted in Figure 3. The ET_B receptor agonist (IRL 1620) at a local concentration of 10^{-8} M constricted both pre- and postglomerular vessels and decreased GBF. The most pronounced vasoconstriction was observed in efferent arterioles, in agreement with earlier findings (22). At a local concentration of $3 \cdot 10^{-5}$ M of the guanylyl cyclase inhibitor (ODQ), a stable reduction of GBF was reached within 15 min. The reduction in GBF was due to a rather homogenous vasoconstriction within the renal arteriolar network ranging from 11% to 19%. The adenosine A_1 receptor agonist (10^{-5} M CPA) induced constriction selectively in preglomerular vessels. In accordance with earlier findings (23,24), the strongest vasoconstriction in response to CPA was observed in the distal segment of the afferent arteriole in close vicinity to the glomerulus. The effects of IRL 1620, ODQ, and CPA were

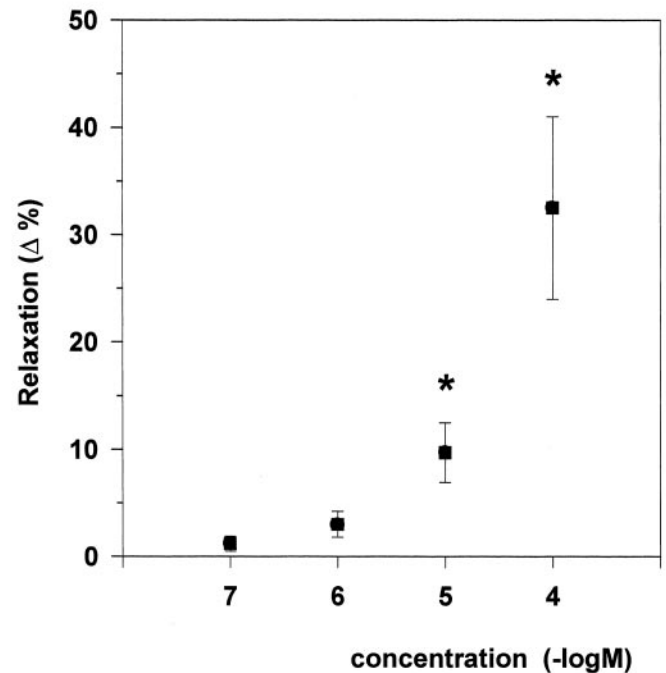
Table 1. Absolute values for vessel diameters, glomerular blood flow (GBF), and MAP for the different experimental groups and for the pooled data of three groups^a

	Group 1 (ET _B Agonist)		Group 2 (ET _B Agonist)		Group 3 (ET _B Agonist)		Group 4 (Guanylyl Cyclase Inhibitor)		Group 5 (A ₁ Agonist)		Groups 1, 4, 5		
	Control	After Y-27632	Control	Before HA-1077	After HA-1077	Control	Before Ro 31-8220	After Ro 31-8220	Control	After Y-27632	Control	After Y-27632	Before Y-27632
ILOB, p, μm	24.0 ± 1.0	30.0 ± 1.5	—	—	—	—	—	—	23.2 ± 1.3	28.9 ± 2.0	25.2 ± 2.0	32.3 ± 2.3	23.0 ± 0.6
ILOB, d, μm	13.1 ± 1.3	18.1 ± 1.3	15.8 ± 0.9	15.8 ± 0.9	18.3 ± 0.9	15.9 ± 0.5	15.8 ± 0.6	17.6 ± 0.6	13.4 ± 1.3	17.9 ± 1.9	15.3 ± 1.5	20.0 ± 1.3	13.9 ± 0.6
AFF, p, μm	10.5 ± 1.0	14.2 ± 0.9	—	—	—	—	—	—	11.5 ± 0.5	15.2 ± 1.0	12.2 ± 1.0	15.3 ± 1.4	13.3 ± 1.1
AFF, d, μm	11.4 ± 0.7	13.9 ± 0.6	—	—	—	—	—	—	10.6 ± 0.6	12.9 ± 0.8	10.6 ± 0.7	13.1 ± 1.0	11.2 ± 0.6
EFF, μm	12.6 ± 1.3	13.1 ± 1.3	12.6 ± 0.4	12.3 ± 0.4	13.9 ± 0.4	13.8 ± 0.7	12.8 ± 0.6	14.3 ± 0.6	11.3 ± 0.9	12.1 ± 0.9	11.8 ± 1.4	12.2 ± 1.5	11.1 ± 0.5
GBF nl/min	64 ± 13	66 ± 14	—	—	—	—	—	—	48 ± 5	84 ± 16	44 ± 5	67 ± 18	45 ± 6
MAP mmHg	125 ± 1	124 ± 1	117 ± 2	119 ± 3	118 ± 3	114 ± 4	109 ± 4	106 ± 3	120 ± 2	123 ± 4	130 ± 4	131 ± 3	128 ± 3
N	6	6	5	5	5	5	5	5	6	6	7	7	19

^a ILOB, interlobular artery; AFF, afferent arteriole; EFF, efferent arteriole; p, proximal; d, distal. Data are means ± SEM.

A

Effects of Y-27632 on interlobular relaxation



B

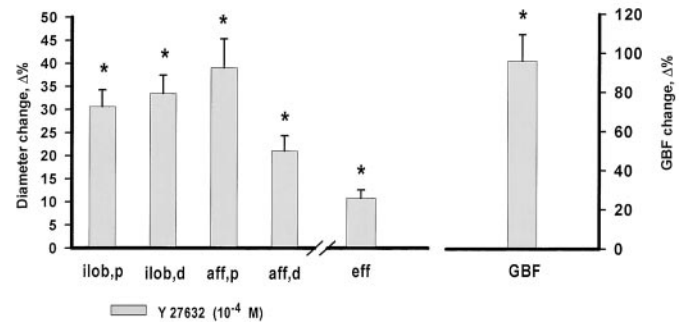


Figure 1. Effect of the Rho kinase (ROK) inhibitor Y-27632 on renal vessels. The ROK inhibitor Y-27632 induced a dose-dependent vasodilation in renal vessels. (A) Percent changes of the diameter of the proximal interlobular artery in response to increasing concentrations of Y-27632. (B) Percent changes of GBF and of diameters for different renal vessels in response to Y-27632 (10^{-4} M). ilob, interlobular artery; aff, afferent arteriole; eff, efferent arteriole; p, proximal; d, distal. Data are mean ± SEM; $n = 3$ (panel A) and $n = 19$ animals (panel B); * $P < 0.05$.

completely reversible, with return of hemodynamic parameters to baseline values after wash out (Table 1).

Effects of ET_B Receptor Agonist (IRL 1620) after ROK and PKC Inhibition

In the presence of the ROK inhibitor Y-27632, the ET_B agonist-induced vasoconstriction was markedly blunted. As

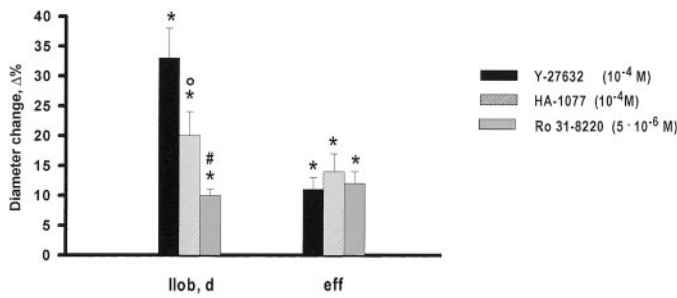


Figure 2. Effect of ROK versus PKC inhibition on renal vessels. Percent changes of the diameter of the distal interlobular artery (illob, d) and of the efferent arteriole (eff) in response to ROK inhibition with Y-27632 (10^{-4} M) or HA-1077 (10^{-4} M) or to PKC inhibition with Ro 31–8220 ($5 \cdot 10^{-6}$ M). Data are mean \pm SEM; $n = 14$ to 23 vessels of $n = 5$ to 19 animals; * $P < 0.05$ significant diameter change; $^{\circ} P < 0.05$ significant difference versus Y-27632; # $P < 0.05$ significant difference versus Y-27632 and HA-1077.

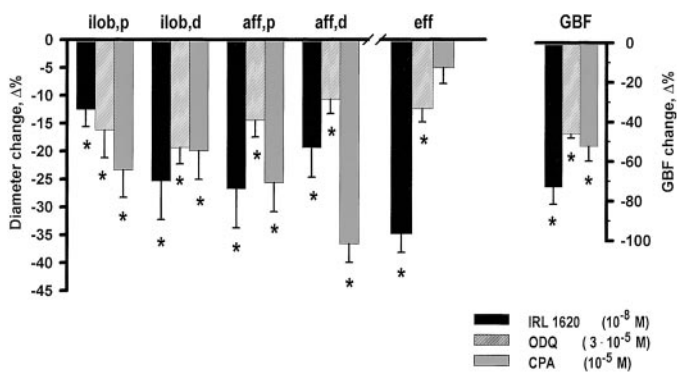


Figure 3. Effect of vasoconstrictors that activate distinct signaling pathways in renal vessels. Percent changes of glomerular blood flow (GBF) and vessel diameters in response to the ET_B receptor agonist IRL 1620 (10^{-8} M), to the guanylyl cyclase inhibitor ODQ ($3 \cdot 10^{-5}$ M), and to the adenosine A_1 receptor agonist CPA (10^{-5} M). Note the different vascular patterns of constriction observed in response to the three different compounds. ilob, interlobular artery; aff, afferent arteriole; eff, efferent arteriole; p, proximal; d, distal. Data are mean \pm SEM; $n = 6$ to 7 animals; * $P < 0.05$.

shown in Figure 4, the same concentration (10^{-8} M) of the ET_B agonist (IRL 1620) as applied in the beginning induced only small changes in GBF and in vessel diameters ($<6\%$; $P > 0.05$) in the presence of the ROK inhibitor Y-27632. A tenfold higher concentration (10^{-7} M) of the ET_B agonist (IRL 1620) was required to obtain a distinct reduction in GBF, whereas vasoconstriction still remained weak ($<17\%$, $P > 0.05$). Importantly, both efferent and preglomerular vasoconstriction in response to the ET_B agonist (IRL 1620) were attenuated by the ROK inhibitor Y-27632 to a similar extent. The structurally different ROK inhibitor HA-1077 (10^{-4} M) blunted ET_B agonist-induced vasoconstriction in pre- and postglomerular vessels to a similar degree as Y-27632 (Figure 5). In contrast, the PKC inhibitor Ro 31–8220 did not significantly affect ET_B agonist-induced vasoconstriction (Figure 5).

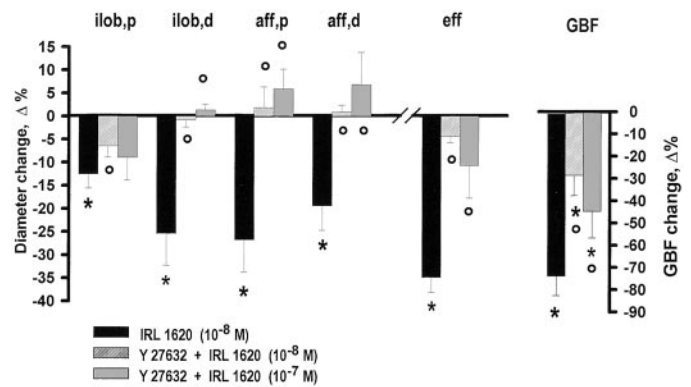


Figure 4. Effect of the ROK inhibitor Y-27632 on ET_B agonist-induced renal vasoconstriction. Percent changes of GBF and vessel diameters in response to the ET_B receptor agonist IRL 1620 (10^{-8} M) in the absence and presence of the ROK inhibitor Y-27632 (10^{-4} M). ilob, interlobular artery; aff, afferent arteriole; eff, efferent arteriole; p, proximal; d, distal. Data are mean \pm SEM; $n = 6$ animals; * $P < 0.05$ significant diameter change; $^{\circ} P < 0.05$ significant effect of Y-27632.

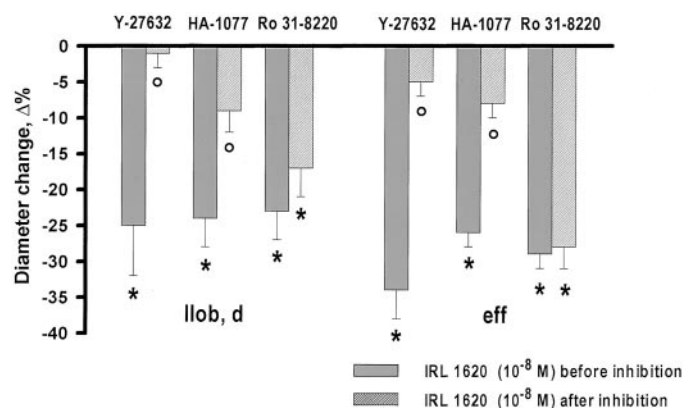


Figure 5. Effect of ROK versus PKC inhibition on ET_B agonist-induced renal vasoconstriction. Percent changes of the diameter of the distal interlobular artery (illob, d) and of the efferent arteriole (eff) in response to the ET_B receptor agonist IRL 1620 (10^{-8} M) in the absence and presence of the ROK inhibitor Y-27632 (10^{-4} M) or HA-1077 (10^{-4} M) or the PKC inhibitor Ro 31–8220 ($5 \cdot 10^{-6}$ M). Data are mean \pm SEM; $n = 6$ to 27 vessels of $n = 5$ to 6 animals; * $P < 0.05$ significant diameter change; $^{\circ} P < 0.05$ significant effect of inhibitor.

Effects of Guanylyl Cyclase Inhibitor (ODQ) and Adenosine A_1 Receptor Agonist (CPA) after ROK Inhibition

After ROK inhibition with Y-27632, vasoconstriction induced by the guanylyl cyclase inhibitor ($3 \cdot 10^{-5}$ M ODQ) was completely abolished both in preglomerular vessels and in efferent arterioles (Figure 6). Likewise, the guanylyl cyclase inhibitor (ODQ) did not induce a significant reduction of GBF in the presence of the ROK inhibitor Y-27632.

The same concentration (10^{-5} M) of the adenosine A_1 agonist (CPA) as applied in the beginning did not alter vessel diameters in the presence of the ROK inhibitor Y-27632 (Fig-

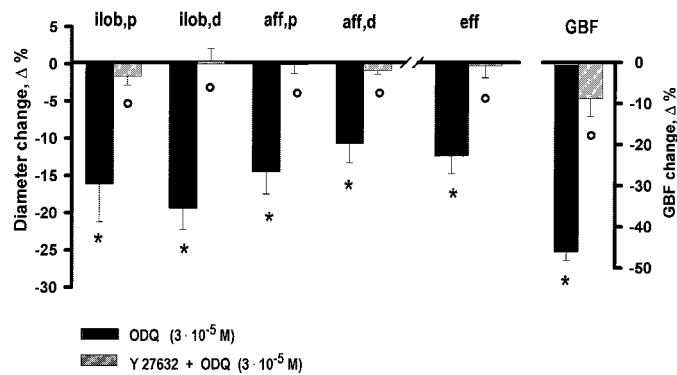


Figure 6. Effect of the ROK inhibitor Y-27632 on renal vasoconstriction induced by guanylyl cyclase inhibition. Percent changes of GBF and vessel diameters in response to the guanylyl cyclase inhibitor ODQ ($3 \cdot 10^{-5}$ M) in the absence and presence of the ROK inhibitor Y-27632 (10^{-4} M). ilob, interlobular artery; aff, afferent arteriole; eff, efferent arteriole; p, proximal; d, distal. Data are mean \pm SEM; $n = 6$ animals; * $P < 0.05$ significant diameter change; ° $P < 0.05$ significant effect of Y-27632.

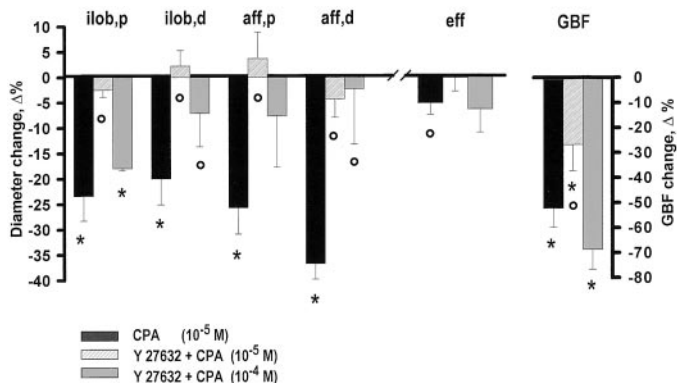


Figure 7. Effect of the ROK inhibitor Y-27632 on A_1 agonist-induced renal vasoconstriction. Percent changes of GBF and vessel diameters in response to the adenosine A_1 receptor agonist CPA (10^{-5} M) in the absence and presence of the ROK inhibitor Y-27632 (10^{-4} M). ilob, interlobular artery; aff, afferent arteriole; eff, efferent arteriole; p, proximal; d, distal. Data are mean \pm SEM; $n = 7$ animals; * $P < 0.05$ significant diameter change; ° $P < 0.05$ significant effect of Y-27632.

ure 7). Specifically, the marked vasoconstriction located in the distal afferent arteriole in response to the adenosine A_1 agonist (CPA) under control conditions was completely abolished after ROK inhibition with Y-27632. However, there was a detectable decrease in GBF, indicating possible vasoconstriction further upstream in larger vessels, *e.g.*, arcuate arteries. A tenfold higher concentration of the adenosine A_1 agonist (10^{-4} M CPA) significantly constricted only the proximal interlobular artery in the presence of the ROK inhibitor Y-27632. At that high concentration, however, the adenosine A_1 agonist (CPA) evoked systemic effects, *i.e.*, an increase in heart rate and severe hypotension, being mainly responsible for the large fall of GBF.

Effects of ROK Inhibition on F-Actin in Renal Vessels

Inhibition of ROK with Y-27632 has been shown to induce disassembly of stress fibers in cultured cells (11). To test whether Y-27632 exerted its renal vasodilator effects via changes in content or structure of filamentous actin in renal arterioles, Y-27632 treated hydronephrotic kidneys were stained for F-actin and examined by confocal microscopy. F-actin intensity and structure did not differ between vessels of Y-27632-treated and control tissue (Figure 8). Treatment with the ROK inhibitor Y-27632 affected actin filament structure in neither vascular smooth muscle cells (arrowheads in Figure 8) nor endothelial cells (arrows in Figure 8).

Discussion

In the present study, we demonstrate that inhibition of ROK blunts the constriction related to distinct signaling pathways in preglomerular vessels as well as in efferent arterioles. The investigation of the role of ROK in vasoconstriction *in vivo*

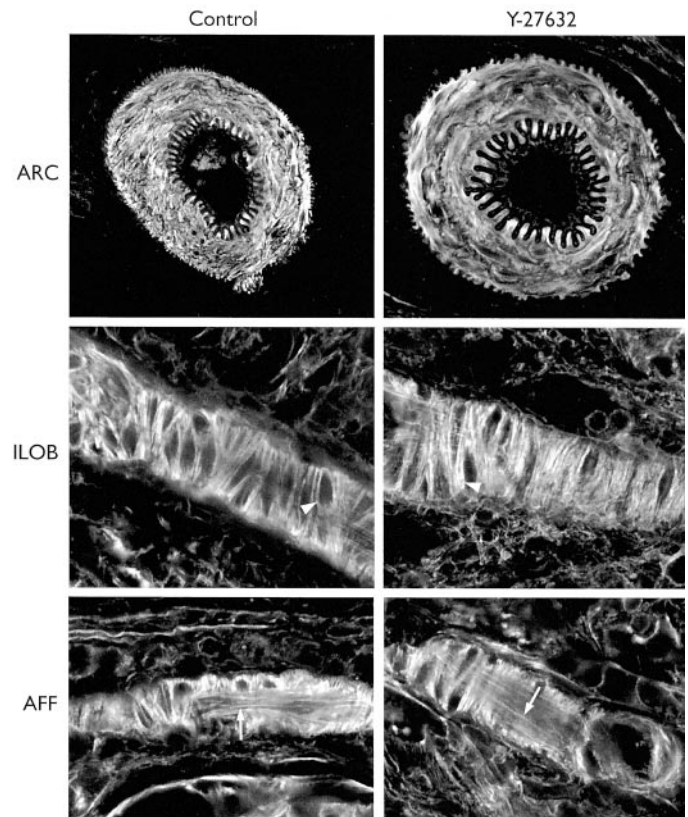


Figure 8. Effect of the ROK inhibitor Y-27632 on F-actin in renal vessels. F-actin distribution in arcuate arteries (ARC), interlobular arteries (ILOB), and afferent arterioles (AFF) of the hydronephrotic rat kidney visualized by confocal microscopy. Images were taken with identical settings of confocal parameters for control and tissue treated with the ROK inhibitor Y-27632 (10^{-4} M). Intensity and distribution of F-actin in renal vessels were similar for control and Y-27632 treated kidneys. Actin filaments around nuclei in smooth muscle cells are marked by arrowheads; actin filaments in endothelial cells are marked by arrows. Magnifications: $\times 130$ (ARC, Control); $\times 300$ (ARC, Y-27632), and $\times 600$ (ILOB, AFF).

became possible with the discovery of specific ROK inhibitors, *i.e.*, HA-1077 (fasudil) (32) and Y-27632 (11). Y-27632 is the most selective ROK inhibitor known, and it blocks MLC kinase only at concentrations above 250 μM (11). Using these two ROK inhibitors it has been shown that inactivation of MLCP significantly contributes to regulation of vasomotor tone and blood flow in several tissues and organs (2). However, the impact of ROK inhibition on the renal vasculature has been addressed in only one study so far, at a time when the molecular target of HA1077 was unknown (32). Intravenous bolus injection of HA1077 increased renal blood flow by about 20% in anesthetized dogs (32).

Endothelin exerts potent renal vasoconstrictor effects *in vivo* through activation of ET_A and ET_B receptors (18,22). Both ET_A and ET_B receptors are known to couple to several types of heterotrimeric G-proteins predominantly leading to PLC activation and intracellular Ca^{2+} mobilization. ET-1 has been demonstrated to increase the amount of GTP-RhoA (33) and to induce most effective phosphorylation of MLC and contraction in bovine aortic VSMC (9). Specifically, the ET_B receptor is able to couple to $\text{G}\alpha_{12/13}$, which in turn activates RhoA (34). Our results demonstrate an important role of ROK in mediating ET_B -induced renal vasoconstriction. ET_B receptor stimulation leads to marked efferent arteriolar constriction, which is blocked by Y-27632 or HA-1077; therefore, ROK-mediated constriction is clearly operative in efferent arterioles. In agreement with our findings, inhibition of the Rho/ROK pathway blunted ET-1-induced vasoconstriction in mammary, mesenteric, penile, cerebral, and coronary arteries (8,35–38). Preventing coronary artery vasospasm in response to ET-1, ROK inhibition protected against myocardial ischemia in rabbits (13,39).

The PKC inhibitor Ro 31–8220 dilated pre- and postglomerular vessels, being equally effective as ROK inhibitors in the efferent arteriole but less effective in the interlobular artery (Figure 2). Thus, part of the basal tone in vessels of the hydronephrotic kidney *in vivo* is due to activation of PKC. Despite the reduction of basal vessel tone, PKC inhibition with Ro 31–8220 failed to prevent ET_B -induced vasoconstriction in our experiments. The ability of PKC to induce constriction of afferent and efferent arterioles has been demonstrated by stimulating PKC with phorbol ester and a diacylglycerol analogue (40). However, selective inhibitors of PKC did not affect norepinephrine- and 20-HETE-induced constriction of isolated interlobar and interlobular arteries, respectively (41,42), suggesting limited or selective activation of PKC by vasoconstrictors. Furthermore, the inability of Ro 31–8220 to inhibit ET_B -induced vasoconstriction clearly demonstrates that the effects of ROK inhibitors Y-27632 and HA-1077 occurred independently of the PKC pathway.

The adenosine A_1 receptor decreases intracellular cAMP levels through G_i protein coupling and has a unique function in the kidney in that it mediates the tubuloglomerular feedback (43). Consistent with this notion, the adenosine A_1 receptor agonist CPA induced marked vasoconstriction in the distal segment of the afferent arteriole, which was sensitive to ROK inhibition in the present study. Besides cAMP, the cyclic

nucleotide cGMP importantly regulates renal vessel tone being the second messenger of natriuretic peptides and NO (44). Inhibition of soluble guanylyl cyclase by ODC induced a strong vasoconstriction of preglomerular vessels and efferent arterioles in our present study, comparable to the effects of NO synthesis blockade by L-NAME (45). Likewise, Trotter *et al.* (46) reported that ODC completely inhibits the renal vasodilation evoked by endogenous NO. Similar to the effect of ROK inhibition on vasoconstriction elicited by reduced cAMP levels, Y-27632 blocked renal vasoconstriction when cGMP levels were lowered by ODC.

There are several targets in the pathways of agonist-induced MLC phosphorylation that can be inhibited by cAMP- and cGMP-dependent kinases (2,3). Thus, changes in intracellular cAMP and cGMP levels result in more or less pronounced changes of vasomotor tone depending on the current degree of MLC phosphorylation. Our observation that decreasing cAMP or cGMP levels failed to induce vasoconstriction in the presence of the ROK inhibitor Y-27632 could be interpreted in a way that both nucleotides interfere with the Rho/ROK pathway. Indeed it has been shown that both cAMP- and cGMP-dependent kinases inhibit the Rho/ROK pathway via serine phosphorylation of RhoA (47–49). On the other hand, in our study ROK inhibition could have lowered the level of MLC phosphorylation to such an extent that reduction of cAMP or cGMP was no longer able to induce vasoconstriction through disinhibition of pathways unrelated to the Rho/ROK pathway. In any case, our results indicate that ROK inhibition impairs vasoconstriction mediated by cAMP and cGMP pathways.

Besides MLCP, ROK also inactivates LIM kinase, thereby inhibiting actin depolymerization (16). Consequently, ROK inhibition has been shown to consistently cause disassembly of stress fibers and a decrease of the F- to G-actin ratio in various cultured cell types, including VSMC (11,50). Matrougui *et al.* (17) demonstrated that ROK inhibition as well as actin filament disruption by cytochalasin B abolished the contractile response of isolated mesenteric arteries to angiotensin II. For the first time, our experiments provide evidence that ROK inhibition results in vasodilation without affecting F-actin organization in vessels *in vivo*. Additional downstream effectors of RhoA (*e.g.*, mDia) (16), which stimulate actin polymerization, might be responsible for the maintenance of the actin cytoskeleton in VSMC during ROK inhibition *in vivo*.

In their first report on Y-27632, Uehata *et al.* (11) have already described that ROK inhibition induces stronger reductions in arterial BP in hypertensive as compared with normotensive rats. Recently, this finding has been extended to humans, in that the increase in forearm blood flow induced by the ROK inhibitor HA-1077 was about twofold higher in hypertensive patients as compared with normotensive subjects (12). There are two findings suggesting a potential therapeutic benefit of ROK inhibition in the renal vasculature. First, lovastatin reduces the level of Rho proteins in renal vessels of hypertensive rats (51). Second, enhanced activation of phospholipase D by angiotensin II in renal VSMC of hypertensive rats is sensitive to blockade of the Rho/ROK pathway (52). The fact that ROK inhibition blunted vasoconstriction in preglomerular ves-

sels as well as in efferent arterioles is of therapeutic relevance and contrasts with the action of Ca^{2+} antagonists, which are without effect on L-type channel-lacking efferent arterioles (53,54).

In conclusion, we demonstrate that ROK inhibitors blunt renal vasoconstriction evoked by distinct signaling pathways without affecting vascular F-actin organization *in vivo*.

Acknowledgments

The authors are indebted to Rudolf Dussel for technical assistance. This work was supported in part by a grant from Società Italiana di Nefrologia (SIN) to Alessandro Cavarape, and by a grant (VIGONI project) from the joint Committee of the Conferenza dei Rettori delle Università Italiane (CRUI) and the Deutscher Akademischer Austauschdienst (DAAD) to Alessandro Cavarape, Ettore Bartoli, and Karlhans Endlich.

References

- Horowitz A, Menice CB, Laporte R, Morgan KG: Mechanisms of smooth muscle contraction. *Physiol Rev* 76: 967–1003, 1996
- Somlyo AP, Somlyo AV: Signal transduction by G-proteins, rho-kinase and protein phosphatase to smooth muscle and non-muscle myosin II. *J Physiol* 522: 177–185, 2000
- Pfizer G: Regulation of myosin phosphorylation in smooth muscle. *J Appl Physiol* 91: 497–503, 2001
- Amano M, Ito M, Kimura K, Fukata Y, Chihara K, Nakano T, Matsuura Y, Kaibuchi K: Phosphorylation and activation of myosin by Rho-associated kinase (Rho-kinase). *J Biol Chem* 271: 20246–20249, 1996
- MacDonald JA, Borman MA, Muranyi A, Somlyo AV, Hartshorne DJ, Haystead TA: Identification of the endogenous smooth muscle myosin phosphatase-associated kinase. *Proc Natl Acad Sci USA* 98: 2419–2424, 2001
- Eto M, Ohmori T, Suzuki M, Furuya K, Morita F: A novel protein phosphatase-1 inhibitory protein potentiated by protein kinase C. Isolation from porcine aorta media and characterization. *J Biochem* 118: 1104–1107, 1995
- Eto M, Kitazawa T, Yazawa M, Mukai H, Ono Y, Brautigan DL: Histamine-induced vasoconstriction involves phosphorylation of a specific inhibitor protein for myosin phosphatase by protein kinase C α and δ isoforms. *J Biol Chem* 276: 29072–29078, 2001
- Batchelor TJ, Sabada JR, Ishola A, Pacaud P, Munsch CM, Beech D: Rho-kinase inhibitors prevent agonist-induced vasospasm in internal mammary artery. *Br J Pharmacol* 132: 302–308, 2001
- Gohla A, Schultz G, Offermanns S: Role for $\text{G}_{12}/\text{G}_{13}$ in agonist-induced vascular smooth muscle cell contraction. *Circ Res* 87: 221–227, 2000
- Lucius CA, Anders A, Steusloff M, Troschka F, Hofmann K, Aktories K, Pfizer G: Clostridium difficile toxin B inhibits carbachol-induced force and myosin light chain phosphorylation in guinea-pig smooth muscle: role of Rho proteins. *J Physiol* 506: 83–93, 1998
- Uehata M, Ishizaki T, Satoh H, Ono T, Kawahara T, Morishita T, Tamakawa H, Yamagami K, Inui J, Maekawa M, Narumiya S: Calcium sensitization of smooth muscle mediated by a Rho-associated protein kinase in hypertension. *Nature* 389: 990–994, 1997
- Masumoto A, Hirooka Y, Shimokawa H, Hironaga K, Setoguchi S, Takeshita A: Possible involvement of Rho-kinase in the pathogenesis of hypertension in humans. *Hypertension* 38: 1307–1310, 2001
- Sato S, Ikegaki I, Asano T, Shimokawa H: Antiischemic properties of fasudil in experimental models of vasospastic angina. *Jpn J Pharmacol* 87: 34–40, 2001
- Navar LG, Inscho EW, Majid DAS, Imig JD, Harrison-Bernard LM, Mitchell KD: Paracrine regulation of renal microcirculation. *Physiol Rev* 76: 425–536, 1996
- Seguchi H, Nishimura J, Toyofuku K, Kobayashi S, Kumazawa J, Kanaide H: The mechanism of relaxation induced by atrial natriuretic peptide in the porcine renal artery. *Br J Pharmacol* 118: 343–351, 1996
- Kaibuchi K, Kuroda S, Amano M: Regulation of the cytoskeleton and cell adhesion by the Rho family GTPases in mammalian cells. *Annu Rev Biochem* 68: 459–486, 1999
- Matrougui K, Tanko LB, Loufrani L, Gorny D, Levy BI, Tedgui A, Henrion D: Involvement of Rho-kinase and the actin filament network in angiotensin II-induced contraction and extracellular signal-regulated kinase activity in intact rat mesenteric resistance arteries. *Arterioscler Thromb Vasc Biol* 21: 1288–1293, 2001
- Cavarape A, Endlich K, Feletto F, Parekh N, Bartoli E, Steinhausen M: Contribution of endothelin receptors in renal microvessels in acute cyclosporine-mediated vasoconstriction in rats. *Kidney Int* 53: 963–969, 1998
- Wayland H, Johnson P: Erythrocyte velocity measurement in microvessels by a two slit-photometric method. *J Appl Physiol* 22: 333–337, 1967
- Gaethgens P: Flow of blood through narrow capillaries: Rheological mechanisms determining capillary hematocrit and apparent viscosity. *Biorheology* 17: 183–189, 1980
- Steinhausen M, Blum M, Fleming JT, Holz FG, Parekh N, Wiegman DL: Visualization of renal autoregulation in the split hydronephrotic kidney of rats. *Kidney Int* 35: 1151–1160, 1989
- Endlich K, Hoffend J, Steinhausen M: Localization of endothelin ET_A and ET_B receptor-mediated constriction in the renal microcirculation of rats. *J Physiol* 497: 211–218, 1996
- Dietrich MS, Endlich K, Parekh N, Steinhausen M: Interaction between adenosine and angiotensin II in renal microcirculation. *Microvasc Res* 41: 275–288, 1991
- Holz FG, Steinhausen M: Renovascular effects of adenosine receptor agonists. *Renal Physiol* 10: 272–282, 1987
- Endlich K, Steinhausen M: Role of kinins and angiotensin II in the vasodilating action of angiotensin converting enzyme inhibition in rat renal vessels. *J Hypertens* 15: 633–641, 1997
- Gabriels G, Endlich K, Rahn KH, Schlatter E, Steinhausen M: In vivo effects of diadenosine polyphosphates on rat renal microcirculation. *Kidney Int* 57: 2476–2484, 2000
- Davies SP, Reddy H, Caivano M, Cohen P: Specificity and mechanism of action of some commonly used protein kinase inhibitors. *Biochem J* 351: 95–105, 2000
- Lanese DM, Conger JD: Effects of endothelin receptor antagonist on cyclosporine-induced vasoconstriction in isolated rat renal arterioles. *J Clin Invest* 91: 2144–2149, 1993
- Loutzenhiser R, Epstein M, Hayashi K, Horton C: Direct visualization of effects of endothelin on the renal microvasculature. *Am J Physiol* 258: F61–F68, 1990
- Loutzenhiser R, Epstein M, Hayashi K, Takenaka T, Forster H: Characterization of the renal microvascular effects of angiotensin II antagonist, *DuP 753*: Studies in isolated perfused hydronephrotic kidneys. *Am J Hypertens* 4: 309S–314S, 1991

31. Welsch T, Endlich N, Kriz W, Endlich K: CD2AP and p130Cas localize to different F-actin structures in podocytes. *Am J Physiol Renal Physiol* 281: F769–F777, 2001
32. Asano T, Suzuki T, Tsuchiya M, Satoh S, Ikegaki I, Shibuya M, Suzuki Y, Hidaka H: Vasodilator actions of HA1077 in vitro and in vivo putatively mediated by the inhibition of protein kinase. *Br J Pharmacol* 98: 1091–1100, 1989
33. Sakurada S, Okamoto H, Takuwa N, Sugimoto N, Takuwa Y: Rho activation in excitatory agonist-stimulated vascular smooth muscle. *Am J Physiol Cell Physiol* 281: C571–C578, 2001
34. Kitamura K, Shiraishi N, Singer WD, Handlogten ME, Tomita K, Miller RT: Endothelin-B receptors activate α_{13} . *Am J Physiol* 276: C930–C937, 1999
35. Matsumura Y, Kita S, Okui T: Mechanisms of endothelin-1-induced potentiation of noradrenaline response in rat mesenteric artery. *Clin Exp Pharmacol Physiol* 28: 3699–37003, 2001
36. Mills TM, Chitale K, Wingard CJ, Lewis RW, Webb RC: Effect of Rho-kinase inhibition on vasoconstriction in the penile circulation. *J Appl Physiol* 91: 1269–1273, 2001
37. Nakamura K, Nishimura J, Hirano K, Ibayashi S, Fujishima M, Kanaide H: Hydroxyfasudil, an active metabolite of fasudil hydrochloride, relaxes the rabbit basilar artery by disinhibition of myosin light chain phosphatase. *J Cereb Blood Flow Metab* 21: 876–885, 2001
38. Sato A, Hattori Y, Sasaki M, Tomita F, Kohya T, Kitabatake A, Kanno M: Agonist-dependent difference in the mechanisms involved in Ca^{2+} sensitization of smooth muscle of porcine coronary artery. *J Cardiovasc Pharmacol* 35: 814–821, 2000
39. Yamamoto Y, Ikegaki I, Sasaki Y, Uchida T: The protein kinase inhibitor fasudil protects against ischemic myocardial injury induced by endothelin-1 in the rabbit. *J Cardiovasc Pharmacol* 35: 203–211, 2000
40. Nagahama T, Hayashi K, Ozawa Y, Takenaka T, Saruta T: Role of protein kinase C in angiotensin II-induced constriction of renal microvessels. *Kidney Int* 57: 215–223, 2000
41. Fetscher C, Chen H, Schafers RF, Wambach G, Heusch G, Michel MC: Modulation of noradrenaline-induced microvascular constriction by protein kinase inhibitors. *Naunyn Schmiedeberg Arch Pharmacol* 363: 57–65, 2001
42. Sun CW, Falck JR, Harder DR, Roman RJ: Role of tyrosine kinase and PKC in the vasoconstrictor response to 20-HETE in renal arterioles. *Hypertension* 33: 414–418, 1999
43. Sun D, Samuelson LC, Yang T, Huang Y, Paliege A, Saunders T, Briggs J, Schnermann J: Mediation of tubuloglomerular feedback by adenosine: Evidence from mice lacking adenosine 1 receptors. *Proc Natl Acad Sci USA* 98: 9983–9988, 2001
44. Gabbai FB, Blantz RC: Role of nitric oxide in renal hemodynamics. *Semin Nephrol* 19: 242–250, 1999
45. Hoffend J, Cavarape A, Endlich K, Steinhausen M: Influence of endothelium-derived relaxing factor on renal microvessels and pressure-dependent vasodilation. *Am J Physiol* 265: F285–F292, 1993
46. Trottier G, Triggle CR, O'Neill SK, Loutzenhisser R: Cyclic GMP-dependent and cyclic GMP-independent actions of nitric oxide in the renal afferent arteriole. *Br J Pharmacol* 125: 563–569, 1998
47. Lang P, Gesbert F, Delespine-Carmagnat M, Stancou R, Pouchelet M, Bertoglio J: Protein kinase A phosphorylation of RhoA mediates the morphological and functional effects of cyclic AMP in cytotoxic lymphocytes. *EMBO J* 15: 510–519, 1996
48. Sauzeau V, Le Jeune H, Cario-Toumanianz C, Smolenski A, Lohmann SM, Bertoglio J, Chardin P, Pacaud P, Loirand G: Cyclic GMP-dependent protein kinase signalling pathway inhibits RhoA-induced Ca^{2+} : Sensitisation of contraction in vascular smooth muscle. *J Biol Chem* 275: 21722–21729, 2000
49. Sawada N, Itoh H, Yamashita J, Doi K, Inoue M, Masatsugu K, Fukunaga Y, Sakaguchi S, Sone M, Yamahara K, Yurugi T, Nakao K: cGMP-dependent protein kinase phosphorylates and inactivates RhoA. *Biochem Biophys Res Commun* 280: 798–805, 2001
50. Sauzeau V, Le Mellionec E, Bertoglio J, Scalbert E, Pacaud P, Loirand G: Human urotensin II-induced contraction and arterial smooth muscle cell proliferation are mediated by RhoA and Rho-kinase. *Circ Res* 88: 1102–1104, 2001
51. Jiang J, Sun CW, Alonso-Galicia M, Roman RJ: Lovastatin reduces renal vascular reactivity in spontaneously hypertensive rats. *Am J Hypertens* 11: 1222–1231, 1998
52. Andresen BT, Jackson EK, Romero GG: Angiotensin II signaling to phospholipase D in renal microvascular smooth muscle cells in SHR. *Hypertension* 37: 635–639, 2001
53. Fleming JT, Parekh N, Steinhausen M: Calcium antagonists preferentially dilate preglomerular vessels of hydronephrotic kidney. *Am J Physiol* 253: F1157–F1163, 1987
54. Hansen PB, Jensen BL, Andreassen D, Skott O: Differential expression of T- and L-type voltage-dependent calcium channels in renal resistance vessels. *Circ Res* 89: 630–638, 2001

See related editorial, "Signaling: Focus on Rho in Renal Disease," on pages 261–264.